ISSN 2277-2685
IJESR/October-December. 2026/ Vol-16/Issue-4/19-24
Chilakala Nagarjun / International Journal of Engineering & Science Research
Full Length Article

Smart Power Quality Monitoring And Harmonic Reduction In Electrical Distribution Systems Using Intelligent Control Techniques

Chilakala Nagarjun[1], Dr L. Kishore[2], Mogarapu Anil kumar[3]
[1]Electrical and Electronics Engineering, Sri Chaitanya Institute of Technology and Research, Khammam, India.
[2]Electrical and Electronics Engineering, Sri Chaitanya Institute of Technology and Research, Khammam, India.
[3]Electrical and Electronics Engineering, Sri Chaitanya Institute of Technology and Research, Khammam, India.
Mail Id: chilakalanagarjuna@gmail.com[1], kishorephd724@gmail.com[2], mogarapuanil@gmail.com[3]

Accepted 15-11-2026
Author(s) Retains the Copyrights of This Article

Abstract
Non-linear loads inject harmonic currents that distort waveforms in distribution systems, and mitigation is most useful when it is triggered by what is measured on the feeder. This paper presents a smart power quality framework in which a per-cycle FFT monitor measures the source-current total harmonic distortion (THD) and enables a shunt active power filter (SAPF) when THD exceeds 5 % for two consecutive cycles. The SAPF combines in-phase current extraction with a sliding mean, hysteresis current control and a DC-link controller, implemented in two versions: a conventional PI controller and an intelligent fuzzy-logic controller. A three-phase 230 V, 50 Hz feeder with a six-pulse rectifier load that steps from 40 A to 60 A is simulated at switching level in Python. Without filtering, the source-current THD is 23.8 %, with 5th, 7th, 11th and 13th harmonics of 18.2, 12.0, 6.4 and 4.9 % of the fundamental. The monitor detects the condition and activates the filter after 40 ms. In steady state, THD falls to 1.51 % with the PI controller and 1.28 % with the fuzzy controller; after the load step it is 4.12 % and 3.88 %. The fuzzy controller gives slightly lower distortion but a larger and slower DC-link transient (731 V peak and 67 ms settling against 707 V and 19 ms for PI), so its advantage is limited. The source is assumed stiff and ideal, the parameters are assumed, and no hardware validation is included.

Keywords: *power quality; harmonic mitigation; shunt active power filter; fuzzy logic control; total harmonic distortion; distribution systems*

Introduction

Power quality (PQ) monitoring and detection have become essential as sensitive power electronic devices, electric-vehicle charging stations, energy storage and distributed generation connect to smart grids and microgrids [1]. Harmonics are a leading concern. Laboratory measurements show that the harmonic currents of several EV chargers can add up when they operate with similar power set-points [2], and high photovoltaic penetration together with EV charging changes harmonic distortion and the hosting capacity of a feeder [3].

The shunt active power filter (SAPF) is a well-established answer: it measures the harmonic current and injects a compensating current, and its performance, efficiency and reliability depend strongly on the control strategy [4], [5]. In practice, monitoring and mitigation are usually designed as separate tasks. A filter that is always active wastes capacity and losses, while a monitor that only reports a problem does not remove it.

This paper links the two functions. The objectives are (i) to implement a per-cycle monitor that measures THD on the source current and enables the SAPF when a threshold is exceeded, (ii) to design the SAPF with a conventional PI DC-link controller and an intelligent fuzzy-logic alternative, and (iii) to compare them in a switching-level simulation with a load step, using THD, individual harmonics, DC-link behavior and switching frequency.

Section 2 reviews related work, Section 3 describes the models and controllers, Section 4 presents and discusses the results, and Section 5 concludes with directions for future research.

Literature Review

Evidence on harmonic sources comes from both measurements and studies of networks. Mazza et al. measured two identical 11 kW bidirectional DC chargers in 100 trials and found that their harmonic contributions add up when the power set-points are similar and tend to cancel as the set-points differ [2]. Dávila-Sacoto et al. studied harmonic distortion and hosting capacity in a feeder with high photovoltaic penetration and EVs, reporting an increase of the third harmonic exceeding 300 % in some cases and a 37.5 % reduction in the

number of vehicles the network could host once harmonics were considered [3]. Owosuhi et al. reviewed the integration of battery storage with PV generation, identified the DC-link voltage, switching and grid-voltage harmonics as notable causes of distortion, and observed that planning models for allocation rarely include the variables needed to curtail harmonic content [6].

For monitoring, Samanta et al. reviewed deep-learning methods for PQ detection and classification, including convolutional networks, autoencoders and recurrent networks, and explained that traditional approaches require large human effort and do not scale well to large systems [1]. Oubrahim et al. reviewed signal-processing and pattern-recognition techniques for characterizing PQ disturbances, in the context of a self-healing smart grid [7].

For mitigation, Hadi et al. reviewed the control of SAPFs, covering current and power calculation methods, PWM control and improvements of PID control, and noted that the THD reduction achieved varied between 0.9 % and 13 % across the techniques considered [5]. Chauhan and Chauhan presented a detailed assessment of active-filter control systems and their key features, stating that the control strategy strongly influences performance, efficiency and reliability [4]. Pichan et al. proposed a deadbeat direct power control for the SAPF with compensation of the digital implementation delay, supported by simulation and experimental DSP tests that showed an improved transient response [8]. Heguig et al. used a predictive current controller for an SAPF connected to a PV generator whose maximum power point is tracked with fuzzy logic [9]. At a broader level, Joshal and Gupta described the use of MPC from converter-level control for power quality to overall energy management in microgrids [10].

Two observations stand out. Monitoring research concentrates on classification accuracy, and mitigation research on the current controller, so that the decision of when to compensate is seldom part of the same design. Second, intelligent controllers are frequently proposed for the SAPF DC-link or current loop, but their benefit over a well-tuned PI controller depends on the metric considered. The present study combines a simple, explainable FFT monitor with the SAPF and compares PI and fuzzy DC-link control under identical conditions, reporting both steady-state distortion and transient behavior.

Materials and Methods

The system of Fig. 1 is a stiff, ideal three-phase source (230 V rms phase voltage, 50 Hz) feeding a six-pulse rectifier load at the point of common coupling (PCC). The load current in each phase is a 120° quasi-square wave of amplitude I_d centered on the voltage peak, smoothed by a 0.3 ms time constant to represent commutation. I_d is 40 A until 0.5 s and 60 A afterwards. The SAPF is a two-level voltage-source inverter with a 3 mH filter inductor, a 3 mF DC-link capacitor, a 700 V reference, and a 2 kΩ resistor that represents DC-link losses. The DC link starts at 640 V to include the pre-charge transient. The system was simulated at switching level in Python 3 (NumPy) with a 4 µs step for 0.9 s. All parameters are assumed values. The block diagrams of Fig. 1 and Fig. 2 use a Simulink-style layout.

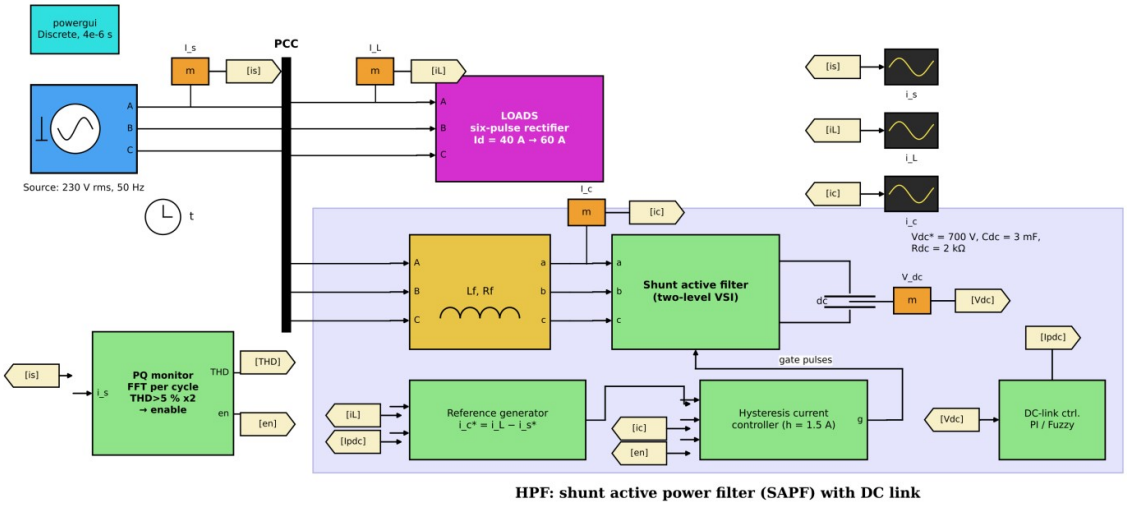

Fig. 1. Simulink-style block diagram of the feeder, non-linear load, SAPF and smart PQ monitor.

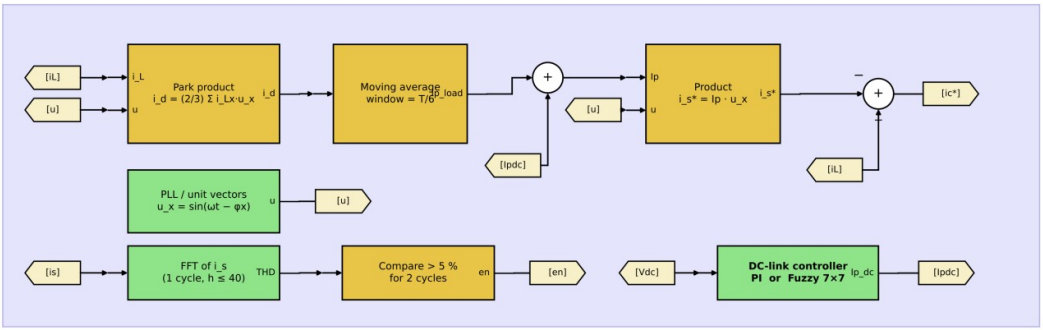

Fig. 2. Harmonic extraction, reference generation and monitoring logic.

Procedures

Step 1: monitoring. At the end of every cycle, the source current of phase a is analyzed by FFT. THD is computed up to the 40th harmonic, and the SAPF is enabled when THD exceeds 5 % in two consecutive cycles:

$$THD = 100\cdot\mathrm{sqrt}(\sum_(h=2)\hat{}(40)\ I_h\hat{}2)/I_1 \quad (1)$$

where I_h is the magnitude of the h-th harmonic of the source current and I_1 that of the fundamental.

Step 2: reference currents. With unit vectors u_x = sin(ωt − φ_x) in phase with the PCC voltage (φ_x = 0, −120°, +120° for phases a, b, c), the in-phase component of the load current and its mean over one sixth of a cycle, which removes the sixth-harmonic ripple of the rectifier, are:

$$i_d = (2/3)\cdot\sum_(x=a,b,c)\ i_Lx\cdot u_x;\quad I_p,load = (6/T)\cdot\int_(t-T/6)\hat{}(t)\ i_d\ dt \quad (2)$$

$$i_s*x = (I_p,load + I_p,dc)\cdot u_x;\quad i_c*x = i_Lx - i_s*x \quad (3)$$

where T is the fundamental period, i_L the load current, i_s *the desired source current, i_c* the compensating-current reference and I_p,dc the correction from the DC-link controller. An ideal phase-locked loop is assumed.

Step 3: current control and power stage. The inverter leg state s_x = ±1 is set by a hysteresis comparator with band h, and the compensating current and DC-link voltage follow:

$$s_x = +1 \text{ if } (i_c*x - i_cx) > h;\ s_x = -1 \text{ if } (i_c*x - i_cx) < -h;\ \text{otherwise unchanged} \quad (4)$$

$$L_f\cdot di_c/dt = v_inv - v_s - R_f\cdot i_c;\quad C_dc\cdot dV_dc/dt = -(1/2)\cdot\sum s_x\cdot i_cx - V_dc/R_dc \quad (5)$$

where v_inv is the inverter voltage referred to the load neutral, v_s the PCC voltage and i_c the compensating current.

Step 4: DC-link controllers. With the error e = V_ref − V_dc updated every 1 ms, the PI controller is $I_p,dc = K_p\cdot e + K_i\cdot\int e\ dt$, with gains obtained from a second-order design (damping 0.7, natural frequency 2π·20 rad/s) and limited to ±30 A. The fuzzy controller is incremental and has two inputs, e/50 and Δe/20, each fuzzified into seven triangular membership functions, an additive 7 × 7 rule base with output index n = i + j (clipped to ±3) and weighted-average defuzzification:

$$I_p,dc(k) = I_p,dc(k-1) + K_f\cdot u_f(e/50,\ \Delta e/20),\quad K_f = 5\ A \quad (6)$$

The fuzzy gain was selected from a short sweep (0.2 to 5 A); the largest value tested gave the fastest DC-link recovery, so the comparison favors neither design by construction but may not be the optimum for the fuzzy controller.

Analysis

Three cases are compared: no filter, SAPF with PI and SAPF with fuzzy DC-link control. THD and the harmonic orders 5, 7, 11 and 13 are computed by FFT over integer numbers of cycles in two windows: 0.2 to 0.5 s (load 40 A) and 0.7 to 0.9 s (load 60 A). DC-link behavior is judged by peak voltage and the time needed to stay within ±1 % of the reference after enabling. The average switching frequency per leg and the RMS currents complete the set of indicators. A THD level of 5 % is used both as the monitor trigger and as a benchmark; limits in standards depend on the short-circuit ratio at the installation and must be checked for a real site.

Results and Discussion

Without compensation, the source current of the rectifier load has a THD of 23.78 %, dominated by the 5th (18.18 %), 7th (12.01 %), 11th (6.35 %) and 13th (4.91 %) harmonics, as expected from a six-pulse rectifier. Fig. 3 shows the phase-a waveforms: the quasi-square load current is converted into a nearly sinusoidal source current by the compensating current.

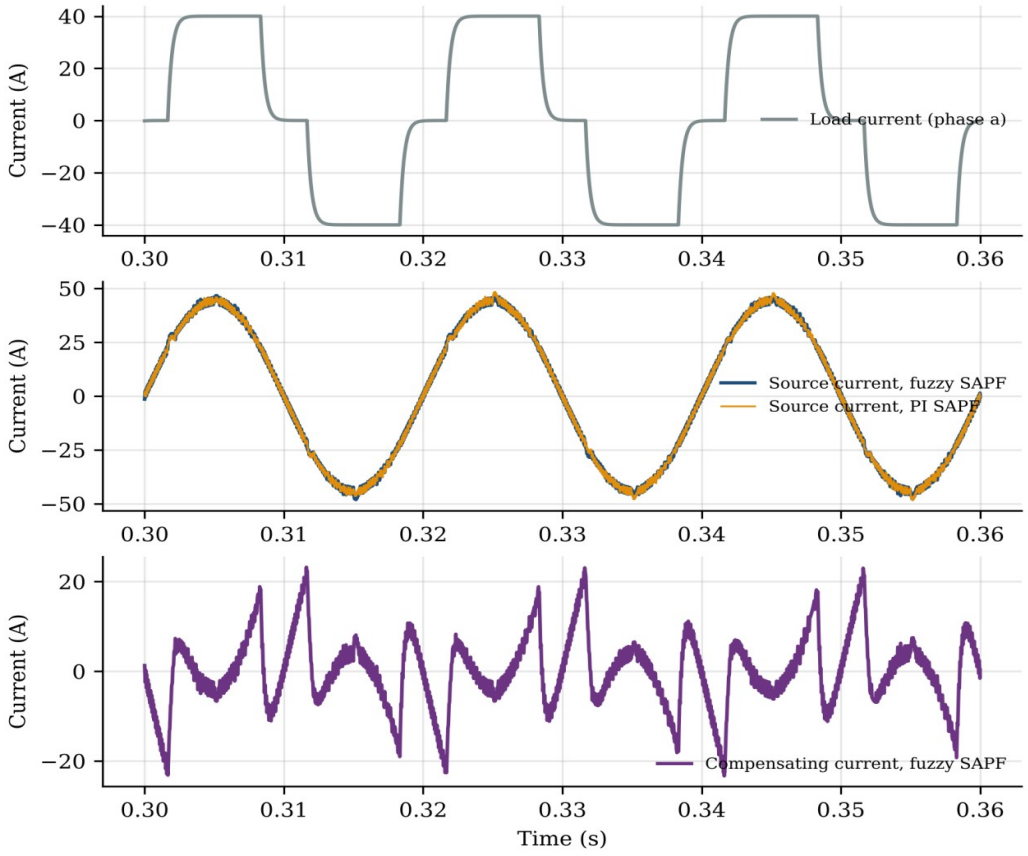

Fig. 3. Phase-a currents between 0.30 and 0.36 s: load current, source current with each SAPF, and compensating current.

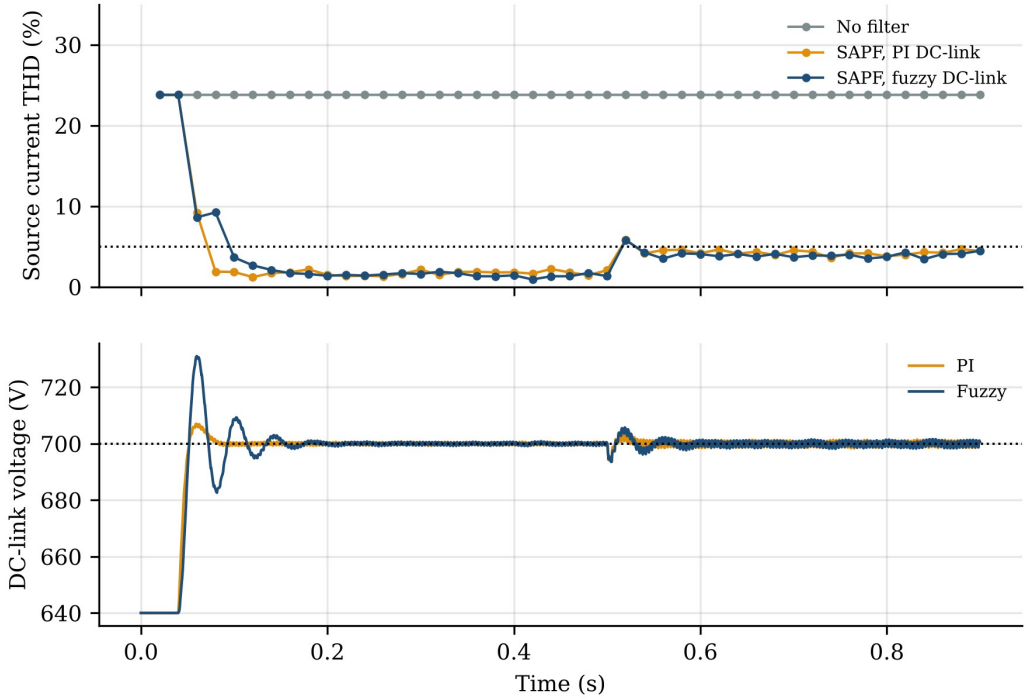

Fig. 4. Per-cycle source-current THD with event-triggered activation, and DC-link voltage.

Fig. 4 shows the monitor in operation. The per-cycle THD of the unfiltered feeder stays at about 24 %. In the two filtered cases the monitor sees two consecutive cycles above 5 % and enables the SAPF at 40 ms; the first monitored cycle afterwards still reads about 9 %, and the THD falls below 2 % after roughly two cycles with the PI controller and five to six cycles with the fuzzy controller, in line with their DC-link transients (lower panel). In the cycle containing the load step at 0.5 s the THD peaks at about 5.8 %, slightly above the threshold, and then settles near 4 %.

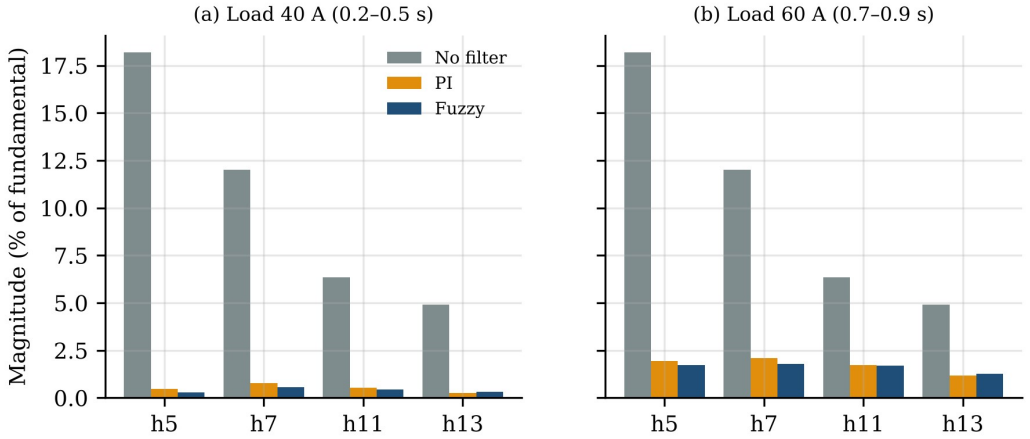

Fig. 5. Source-current harmonic spectrum at (a) 40 A and (b) 60 A load.

Fig. 5 give the quantitative results. At the 40 A load, the SAPF reduces the THD from 23.78 % to 1.51 % (PI) and 1.28 % (fuzzy), a reduction of about 94 %, and each of the four dominant harmonics falls below 1 % of the fundamental. After the load step to 60 A, the THD is higher (4.12 % and 3.88 %), although still below the 5 % benchmark, and the harmonic components rise to about 1.2 to 2.1 %. A plausible explanation is that the larger load-current edges require a faster compensating-current change than the 3 mH inductor can deliver with the available DC-link voltage, so tracking errors at the edges grow; this was not isolated by a separate experiment. The source RMS current falls slightly (from 47.89 to about 47.0 A at 60 A) because the harmonic content is removed from the supply.

shows that the difference between the two controllers is small and mixed. The fuzzy version gives slightly lower THD at both load levels (differences of 0.23 and 0.24 percentage points), but its DC-link transient is worse: 4.4 % overshoot and 67 ms settling against 1.0 % and 19 ms for the PI controller. The reaction to the load step is nearly identical (6.0 V against 6.6 V deviation) because the load-power feed-forward term in the reference calculation absorbs most of the disturbance. The switching frequency (about 4.7 to 4.8 kHz) and compensator RMS current are essentially equal. The gain of the fuzzy controller was tuned in a limited sweep, so a better-tuned design might narrow the DC-link gap; with the present tuning, the PI controller is the better choice for DC-link regulation, and the intelligence of the fuzzy controller does not bring a clear overall advantage.

These findings should be read against the literature with care. Hadi et al. reported that THD reductions across SAPF control techniques lie between 0.9 % and 13 % [5], but those numbers refer to other systems and metrics. The statement that the control strategy influences performance and reliability [4] is supported in the sense that the DC-link controller changed the transient behavior but not the steady-state spectrum in a major way. The deadbeat approach with delay compensation of Pichan et al. targets transient response [8], and the higher THD after the load step in this study indicates that current-slew limits are the place where such methods could help. The monitor used here is a plain FFT, much simpler than the deep-learning classifiers reviewed by Samanta et al. [1]; it answers only one question (is THD too high?), not which disturbance occurred. The loads considered are consistent with the harmonic spectra associated with rectifier-type equipment, as in EV chargers and PV inverters studied in [2], [3], [6], but multiple interacting sources were not simulated. Finally, because the source is stiff and ideal, voltage distortion and resonance at the PCC, which are important in real feeders, are not captured.

Conclusion and Future Work

A smart power quality scheme was built in which a per-cycle FFT monitor enables a shunt active power filter when source-current THD exceeds 5 % for two cycles. In a switching-level simulation of a six-pulse rectifier load, the unfiltered THD of 23.78

% was reduced to 1.51 % with a PI DC-link controller and 1.28 % with a fuzzy controller at 40 A, and to 4.12 % and 3.88 % after a step to 60 A, with activation after 40 ms. The fuzzy controller gave marginally lower distortion but a larger and slower DC-link transient, so the intelligent controller was not clearly superior to a PI design in this setting.

The contribution is an explicit link between monitoring and mitigation, together with a transparent comparison of two DC-link controllers under identical conditions. The scope is limited by the assumed parameters, the ideal and stiff source, the single load type and the lack of hardware tests. Future work should include source impedance and voltage distortion, deadbeat or predictive current control to improve transient tracking, monitors that classify disturbances rather than only measuring THD, interacting EV and PV harmonic sources, a release criterion for switching the filter off, and experimental validation on a DSP or FPGA platform.

References

[1] Samanta, I. S., Panda, S., Rout, P. K., Bajaj, M., Piecha, M., Blazek, V., & Prokop, L. (2023). A comprehensive review of deep-learning applications to power quality analysis. *Energies*, *16*(11), 4406. https://doi.org/10.3390/en16114406

[2] Mazza, A., Benedetto, G., Bompard, E., Nobile, C., Pons, E., Tosco, P., Zampolli, M., & Jaboeuf, R. (2023). Interaction among multiple electric vehicle chargers: Measurements on harmonics and power quality issues. *Energies*, *16*(20), 7051. https://doi.org/10.3390/en16207051

[3] Dávila-Sacoto, M., González, L. G., Hernández-Callejo, L., Duque-Perez, Ó., Zorita-Lamadrid, Á. L., Alonso-Gómez, V., & Espinoza, J. L. (2023). Harmonic distortion and hosting capacity in electrical distribution systems with high photovoltaic penetration: The impact of electric vehicles. *Electronics*, *12*(11), 2415. https://doi.org/10.3390/electronics12112415

[4] Chauhan, S. K., & Chauhan, V. S. (2024). A comprehensive review on power quality issues and disturbances mitigation through shunt active power filters. *International Journal of Applied Power Engineering*, *13*(4), 844–852. https://doi.org/10.11591/ijape.v13.i4.pp844-852

[5] Hadi, A., Thjeel, E., & Nahar, A. (2022). A review of control technique applied in shunt active power filter (SAPF). *Engineering and Technology Journal*, *40*(8). https://doi.org/10.30684/etj.v40i8.2116

[6] Owosuhi, A., Hamam, Y., & Munda, J. (2023). Maximizing the integration of a battery energy storage system–photovoltaic distributed generation for power system harmonic reduction: An overview. *Energies*, *16*(6), 2549. https://doi.org/10.3390/en16062549

[7] Oubrahim, Z., Amirat, Y., Benbouzid, M., & Ouassaid, M. (2023). Power quality disturbances characterization using signal processing and pattern recognition techniques: A comprehensive review. *Energies*, *16*(6), 2685. https://doi.org/10.3390/en16062685

[8] Pichan, M., Seyyedhosseini, M., & Hafezi, H. (2022). A new deadbeat-based direct power control of shunt active power filter with digital implementation delay compensation. *IEEE Access*, *10*. https://doi.org/10.1109/ACCESS.2022.3188685

[9] Heguig, L., Mesbahi, N., & Guettaf, Y. (2025). Control of shunt active power filter for power quality improvements with PV system using MPC approach. *International Journal of Power Electronics and Drive Systems*, *16*(1), 278–286. https://doi.org/10.11591/ijpeds.v16.i1.pp278-286

[10] Joshal, K. S., & Gupta, N. (2023). Microgrids with model predictive control: A critical review. *Energies*, *16*(13), 4851. https://doi.org/10.3390/en16134851